Frio II Brine Pilot:
Report on GEOSEQ Activities
September 2007

T.M. Daley, B.M. Freifeld, J.B. Ajo-Franklin, C. Doughty, S.M. Benson[1],

Lawrence Berkeley National Laboratory, Earth Sciences Division,
[1]Stanford University, Global Climate and Energy Project

Abstract

LBNL's GEOSEQ project is a key participant in the Frio II brine pilot studying geologic sequestration of CO_2. During the injection phase of the Frio-II brine pilot, LBNL collected multiple data sets including seismic monitoring, hydrologic monitoring and geochemical sampling. These data sets are summarized in this report including all CASSM (continuous active source seismic monitoring) travel time data, injection pressure and flow rate data and gaseous sampling and tracer data. Additional results from aqueous chemistry analysis performed by the U. S. Geological Survey (USGS) are summarized. Post injection modification of the flow model for Frio II is shown. These modifications are intended to facilitate integration with the monitoring data and incorporation of model heterogeneity. Current activities of LBNL's GEOSEQ project related to the Frio II test are shown, including development of a new petrophysical model for improved interpretation of seismic monitoring data and integration of this data with flow modeling.

1. Introduction

The purpose of this report is twofold: (1) to summarize the data collected by LBNL during the injection phase of the Frio-2 brine pilot experiment, including data generated from LBNL's U-tube (fluid and/or gas samples) by other participants of Frio II; and (2) to report on the status of LBNL's current activities related to the Frio experiment. Additionally, information on downhole instrumentation conditions discovered during removal of monitoring equipment is included. The data collected are in three main categories, (1) seismic monitoring, (2) geochemical sampling, and (3) modeling of flow and transport, with figures and tables summarizing the data in Appendices A, B, and C, respectively.

Current activities, in addition to continuing analysis and integration of the data collected, are focused on understanding the rock physics (petrophysics) relating seismic properties to changes in CO_2 saturation. Figures from our current petrophysical modeling are shown in Appendix D. We feel this is a very important issue for the sequestration community. The reason for this focus is that it has now been demonstrated that storage in brine reservoirs, such as Frio, Sleipner, and others, can be monitored and mapped via seismic methods (e.g., surface seismic, VSP, crosswell). The seismic responses being monitored may be either changes in velocity or amplitude (i.e., attenuation). However, a key step to quantifying the amounts of CO_2 stored in any given rock volume is relating the seismic response to CO_2 saturations. With this relationship, and given knowledge of the reservoir rock matrix, the mass of CO_2 stored in a given rock volume can then be estimated. The ability to generate a mass estimate using seismic methods may be one of the key components in a Monitoring and Verification program required for commercial operators to demonstrate to regulators and the public the safe and effective operation of a geologic carbon sequestration storage program.

The initial rock physics models used in interpreting Frio I (Daley, et al., 2007) are being updated with a new approach known as "patchy saturation" models. The model formulation and rationale are described here. Our plan for future work is to collect core measurements to calibrate the rock physics and then use this petrophysical model to combine the flow modeling with geophysical forward modeling in an iterative forward solution of both flow and geophysical properties. The goal is both quantitative estimates of CO_2 saturation and semi-automated updates of flow models using geophysical modeling.

2. Frio II Pilot Background

2.1. Overview

The Frio brine pilot site, near Houston, Texas, was the site of the Frio I injection test in 2004, as described in Hovorka, et al., 2005. In 2006, the Frio II pilot program conducted a second CO_2 injection of about 320 tons, carried out in the Blue sand at a depth of about 1650 m in an Oligocene fluvial sandstone. The Blue sand is high porosity (~34%), high permeability (3-4 darcies), dipping (11-15 degree), with numerous overlying shale seals including the thick Anahuac shale. The injection zone is believed to be in a small fault

block near the edge of a salt dome. The brine reservoir had pressure of about 16.5 Mpa (165 bars) and temperature of about 55°C. At these conditions the CO_2 injected was in supercritical state. The overall goals of the Frio-II brine pilot experiment include studying storage permanence, quantifying residual saturation and dissolution, conducting post-injection monitoring under stable conditions, and studying buoyancy in a thick sand.

2.2. LBNL Role at Frio-II

As an integral member of the Frio research team, LBNL was responsible for operation of the U-tube geochemical sampling system and CASSM (continuous active source seismic monitoring) equipment during the completion of active injection and during follow-up monitoring. Both the U-tube and CASSM were designed at LBNL (Freifeld et al., 2005; Daley, et al., 2007). The U-tube provided fluid and gas samples at the surface while maintaining in-situ pressure conditions. These samples were provided to other researchers on the Frio team, with gas content analysis performed at LBNL. The CASSM data provided real-time monitoring of CO_2 induced seismic velocity changes. These CASSM data were used on-site to track the progress of the CO_2 plume between injection and observation wells and are being analyzed and interpreted by LBNL. LBNL also conducted flow modeling using TOUGH2 and assisted in the selection and operation of pressure and flow monitoring instrumentation.

3. Frio-II Injection Phase Data Summary

3.1. Continuous Active Source Seismic Monitoring (CASSM)

The initial CASSM results from Frio II have been presented and published (Daley, et al., 2007) and will be only summarized here. The CASSM experiment was a unique design which required development of novel instrumentation (including the ”piezo-tube” seismic source, patent pending). The continuous monitoring of crosswell seismic response provided information on the spatial and temporal variation of the CO_2 plume as it migrated. A seismic monitoring experiment such as the Frio-II CASSM generates gigabytes of data which can be processed and analyzed in various ways. The initial and primary data set is crosswell travel time change (delay time) as a function of calendar time. These data are shown in Appendix A. Most notable is Figure A1 which shows the relationship of data from key sensor depths over the injection time. As discussed in Daley, et al. (2007), the buoyancy driven flow of the CO_2 within the reservoir is demonstrated and constrained by the early detection at sensor depth 1650 m, before CO_2 arrived in the observation well. In the updated data plot (Figure A1) the data from sensor 1650 now shows a clear reduction in seismic response following the end of injection. The rate of decrease is similar to the pre-breakthrough rate of increase and is interpreted as being related to the rate of change of the CO_2 plume saturation-thickness product. Other sensors do not show a similar post injection change, indicating that plume changes are localized to the top of reservoir. Two sensors, at 1648 m and 1654 m, have data still under study for possible modification of travel-time picks. The CASSM data, with 15

minute sampling, combined with U-tube fluid sampling on 1-2 hour intervals, provide key constraints on CO_2 flow in the brine reservoir at scales not previously measured.

3.2. Downhole Instrumentation Condition

The CASSM experiment ended about a week after injection ceased, due to failure of a downhole electrical connection within the sensor string (deployed in the observation well). Additional information regarding the response of the instrumentation material to long-term deployment was obtained when the system was removed from the wells in July 2007 and is being analyzed. The sensor cable's downhole electrical connection used a buna-N (nitrile rubber) O-ring, which is a likely cause of failure. Another potential cause is small nicks in the O-ring sealing surface which were observed before installation. The cable itself was a polyurethane which survived, however part of the hydrophone outer mold which was not polyurethane had significant damage apparently due to long-term exposure to CO_2-rich fluids. The seismic source cable was a standard coaxial cable with an additional outer polyurethane outer jacket. Upon removal from the injection well, a cut was observed in the outer jacket which allowed well fluid, including CO_2, to penetrate between layers. However, the source cable maintained its electrical integrity during the injection and this cut may have occurred during removal. Additionally, during removal, the injection tubing was observed to have a 0.2" hole at about 550 m depth. This tubing was standard steel, newly purchased for the Frio project.

3.3. Hydrological Monitoring and U-tube Geochemical Sampling

3.3.1. Injection Pressure and Flow Rate

Figure B1 shows the CO_2 mass injection rate and the bottom-hole pressure throughout the Frio II injection. The total mass of CO_2 injected is estimated to be 320 metric tons. The flow rate is seen to oscillate up and down reflecting difficulty in the pumps and heat exchanger to maintain steady pressure/flow conditions on the CO_2 injection stream. The long pause in the middle of the injection was caused by a failed seal on a compressor pump, which needed to be replaced before injection could continue. The bottomhole pressure in the injection well increases only approximately 40 PSI (maximum) (2.7 bar) during the injection reflecting the high permeability of the Blue Sand formation.

3.3.2. U-Tube Sampling

The U-tube was developed specifically for the Frio I pilot test (Freifeld, et al., 2005) to provide uncontaminated samples of fluid and gas at near *in situ* conditions. For Frio-II both the injection and observation wells were fitted with U-tube samplers, installed via production tubing. The instrumentation deployment was unique as the U-tube installation was fully integrated with the CASSM equipment. Samples collected from the injection and observation well have been summarized in Table B1. Aqueous splits from the U-tube were provided to the USGS (under the supervision of Yousif Kharaka) for analysis of aqueous chemistry (pH, EC, Eh, cations and anions) and several samples were selected for detailed analysis of organics and metals. Aqueous chemistry and results for some

metals have been summarized in Table B2. More detailed organic and metal analysis results are still pending.

3.3.3. Gas Sampling and Analysis

Gas splits were collected and a portion was analyzed onsite using a quadrupole mass spectrometer (MS) (Omnistar, Pfeiffer Vaccum Systems) (Freifeld and Trautz, 2006). Figure B2 shows the relative concentrations of CH_4 and CO_2 normalized to one. The primary constituent that is corrected for is N_2, which is residual in the sampling tubes as part of the purging and sampling procedure. Figure B3 shows qualitative breakthrough elution curves for perfluorocarbon tracers (PFTs), Kr, and SF_6 which were also analyzed using the field mass spectrometer.

Gaseous splits were collected onsite by Jim Underschultz from CO2CRC, Australia for analysis of perdeuterated methane tracer. Perdeutrated methane ($^{12}CD_4$) is the end-member isotopologue of $^{12}CH_4$ and, as such, offers the best gas chromatographic (GC) resolution from methane. CD_4 is GC baseline-resolved on a molecular sieve GC capillary column when doped in CH_4 with a GCMS detection limit of 0.05 part per billion volumetrically (ppbv) (signal-to-noise ratio of 2 for m/z 20.06 at 1000 resolution), which is similar to the sensitivity achieved by MS-MS (Mroz et al., 1989a). CD_4 has been used sparingly in airborne-based studies (Mroz et al., 1989b; NPS, 1989) where the extremely low natural level of CD_4 at $1.3*10^{-16}$ volumetrically (Mroz et al., 1989a) offers minimal ”background” in mass spectral detection.

During Frio II, CD_4 was used for the first time to our knowledge as a tracer in the sub-surface. Sixteen hours after the commencement of the CO_2 injection, CD_4 (27 g) was injected as a front to ~100-fold excess of Kr and Xe. At the monitoring well, 30 m up-dip of the injection well, Xe unexpectedly arrived with CO_2 breakthrough 48.3 hours after CO_2 injection began, but only 31.9 hours after the injection of the tracers (Figure B4). The first gas sample for CD_4 analysis was taken after another 9.4 hours while the last sample was taken at 207.2 hours after CO_2 injection. Maximum CD_4 concentrations (up to of 92 ppbv) were observed between 57.7 and 69 hours. The CD_4 concentration elution profile follows closely that of Kr and Xe (not shown), suggesting very similar migration pathways for CD_4 and the noble gases between the injection and the monitoring wells. Despite the narrow injection pulse for CD_4, it was still detectable 1 week after introduction at concentration levels of a few to sub-ppbv, indicating dispersion.

3.3.4. Downhole Sampling Equipment Condition

The observation well U-tube was fully operational and facilitated sampling throughout the course of injection (at 1-2 hour intervals) and in the weeks and months following. Shortly after the conclusion of the active injection phase of Frio II, the injection well U-tube had a downhole failure. This was initially noted because coarse sand was able to travel up the U-tube, indicating the sintered metallic inlet filter had experienced a failure. While an exact cause of this failure has not been determined, other observations of deterioration indicate that the CO_2/brine environment may have contributed to premature

failure of the weld that attaches the sintered metallic filter inlet to the solid sampling tube. The other observations of deterioration include a 0.2 inch hole in the injection tubing at 1110 m depth along with 12 pinholes discovered in the observation well stainless steel U-tube sampling lines between 1370 and 1670 m.

4. Flow Modeling

Initial modeling with TOUGH2 was used to guide the design of the Frio II experiment. Figure C1 in Appendix C shows a view of the expected plume growth, based on well log and core information from the injection well. It is notable that the model based on this fine-scale information did not capture the true response of the injected plume. As stated in Doughty, et al., (2007) "only through the injection and monitoring of CO_2 could the impact of the coupling between buoyancy flow, geologic heterogeneity, and history-dependent multi-phase flow effects truly be appreciated." The geophysical and geochemical monitoring of the injection site is thus key to constraining and modifying the flow models. This integration between modeling and monitoring is one of the key components of the ongoing Frio analysis within the GEOSEQ project. A new 3D model of the Blue Sand is being developed, to improve on shortcomings of the previous model and to facilitate comparison with the different types of monitoring data that were collected during and after CO_2 injection. Specifically, the new model has higher lateral spatial resolution (1 m instead of 2 m near the wells; 2 m instead of 5 m in the neighborhood of the wells) and is oriented with one axis parallel to the line joining the injection and observation wells. The higher resolution will decrease numerical dispersion and facilitate incorporating heterogeneous porosity and permeability distributions. The new orientation will enable efficient comparison of model results to real-time seismic data. This model is shown in Appendix C, Figure C2. Methodologies for implementing seismic data as a constraint on the flow model are being developed and tested.

5. Current Activity: Improving Seismic Petrophysical Models

A key component of the Frio experiment data analysis is development of a rock physics model relating seismic velocity to CO_2 saturation. The estimation of CO_2 saturation from seismic measurements affords one of the only MMV techniques capable of detecting CO_2 movement beyond the zone immediately surrounding the borehole. Rock physics models capable of predicting the change in geophysical properties induced by CO_2 provide a link between multiphase flow simulation and seismic modeling; module [B] in Figure D1 shows the role which petrophysical modeling plays in our integrated predictive framework.

The rock physics formulations we are currently exploring fall into the broad class of fluid substitution models; given the properties of a water-saturated or dry rock, these models attempt to predict the change in geophysical properties induced by adding a second fluid phase, in this case supercritical CO_2. Significantly, such models do not attempt to predict rock properties *ab initio* from information on frame mineralogy or pore structure but only consider the effects of changing fluid saturation. Our prior work on saturation effects was

based upon the model of Brie et al. (1995); in this section we will describe recent refinements of our rock property formulation, bounds on the uncertainty of saturation estimates from crosswell/VSP seismic measurements, and future research tasks which may reduce this uncertainty.

All fluid substitution models rely upon accurate property estimates for the constituent fluid phases. As part of improving the quality of our seismic estimates of CO_2 saturation, we have implemented new property calculators for both supercritical CO_2 and brines which can accommodate *in situ* reservoir temperatures and pressures. Our pure CO_2 property model is based upon the combined NIST fluid standard (Lemmon et.al., 2005) and includes bulk modulus, density, viscosity, and phase state for temperatures between 10 and 150 ^oC and pressures up to 100 MPa. The resulting CO_2 properties compare favorably to the EOS model of Altunin (1975) used in the TOUGH2/ECO2N flow simulator. Figure D2 shows the dependence of density [A] and bulk modulus [B] on P/T state with the *in situ* reservoir conditions at Frio (~15 MPa, ~55 ^oC), Sleipner (~10.7 MPa, ~37 ^oC), and the SECARB Phase III demonstration site at Cranfield (~30 MPa, ~125 ^oC) superimposed as black squares. Brine properties are calculated using the formulation of Batzle and Wang (1992). Unlike ECO2N, we treat the two fluid phases as immiscible; at the relevant P/T state, dissolved CO_2 in the brine phase should not significantly alter seismic properties. In contrast to our use of the NIST model, recent work by Carcione et.al. (2006) relies on a simple van der Waals (VDW) equation for supercritical CO_2 properties, a choice which yields errors of ~200 kg/m^3 at the P/T state present at Frio; this disagreement is highlighted in Figure D3 which shows the pressure dependence of density (panel A) and P-wave velocity (panel B) for both models at *in situ* Frio formation temperatures. As can be seen, the VDW model (dashed curve) predicts significantly lower densities and velocities than the NIST model (solid curve) at measured down-hole pressures (black squares).

The primary objective of our petrophysical estimation tool is a reliable approach to map changes in CO_2 saturation to changes in observable seismic signatures, a process which requires information on the properties of the rock frame, the characteristics of the fluid phases, their volumetric fractions, and finally their spatial distributions within the rock volume. Previous analysis of the Frio I dataset (Daley, 2007) relied on application of the heuristic model proposed by Brie et al. (1995); this model suffers from several limitations, the most serious of which is the use of an *ad hoc* fitting parameter with no physical basis. Tuning this parameter in the absence of detailed log or core scale calibration measurements allows generation of a wide range of saturation vs. modulus relationships, some of which violate hard bounds on the properties of fluid saturated materials. Another limitation of the Brie et al. model is its neglect of seismic attenuation which is associated with compressible fluids occupying macroscopic patches.

Based on these observations, we have adopted the model of White (1975), including the corrections made by Dutta & Seriff (1979), for the prediction and interpretation of seismic property changes due to partial CO_2 saturation. White's model assumes a homogeneous rock frame with spherical patches of dimension $\boldsymbol{r}$ saturated with a second fluid phase, in our case supercritical CO_2. The model assumes that the seismic

wavelength is larger than the characteristic patch dimension and reduces to the traditional Gassmann model in cases where only a single fluid phase is present. While ***r*** is sometimes used in practice as a fitting parameter, much like the coefficient in the Brie et al. model, values of ***r*** in White's model correspond to a physical quantity which could be measured in an appropriate laboratory experiment.

Panel A of Figure D4 compares White's model (WDO), to three other poroelastic models commonly used to predict the properties of rocks partially saturated with CO_2. The elastic properties of the rock frame were selected from log and core information collected in the Blue Sand formation (base V_p = 2700 m/s, base V_s = 1200 m/s, permeability = 2 darcies). CO_2 and brine properties were calculated for *in situ* reservoir pressures and temperatures (P = 15 MPa, T = 55 ^oC). All curves show the change in V_p as a function of CO_2 saturation. The blue curve corresponds to the physical case where CO_2 is well-mixed with brine on the pore scale while the green curve (the Biot-Gassmann-Hill model) is the quasi-static prediction for a partially saturated medium with macroscopic patches. Depending on the choice of ***r***, the WDO model ranges between these curves; the black lines in Figure D4 indicate the WDO predictions for CO_2 patch radii of 2.5 cm (dashed) and 15 cm (solid). In practice, we typically have no prior knowledge of ***r*** which leads to considerable uncertainty when attempting to estimate CO_2 saturation from changes in seismic velocity. For a decrease in P-wave velocity of 200 m/s (dashed cyan line), CO_2 saturations might be anywhere between 4 and 40% depending on the choice of patch size. Larger patch dimensions exhibit a quasi-linear relationship between V_p and CO_2 saturation whereas pore-scale mixing is very sensitive to low CO_2 saturations but insensitive to variations beyond 25%. Selecting the appropriate mixing length scale is required to quantitatively predict saturation from seismic measurements. Conceivably, this value could come from either calibration experiments (on the core or log scale) or from the field scale measurement of secondary properties such as P-wave attenuation or electrical conductivity.

The WDO model, in addition to predicting a decrease in velocity due to partial CO_2 saturation, predicts a peak in P-wave attenuation at intermediate saturations as shown in panel B of Figure D4. This attenuation peak is due to relative fluid motion across the boundaries of the postulated macroscopic patches; the peak's location is determined by ***r,*** the seismic frequency (f) used within the imaging experiment, and several secondary material properties including permeability. The difference in character between the V_p and attenuation response profiles suggests that a combination of the two properties might be useful for estimating both CO_2 saturation and patch dimensions. Figure D5 shows the WDO model for different patch dimensions in the form of a cross-plot between change in V_p (x axis) and change in P-wave attenuation (y axis). Each curve corresponds to a single WDO patch dimension evaluated for a range of CO_2 saturations with ***r*** ranging between 2.5 cm (blue) to 15 cm (green). Significantly, the curves do not intersect at low to mid saturations, i.e., the combination of V_p and attenuation should yield a unique estimate of both ***r*** and CO_2 saturation without requiring a calibration dataset. At high saturations, corresponding to the left side of Figure D5, the WDO models converge to similar V_p/attenuation pairs, thus reintroducing ambiguity between seismic response and CO_2 saturation.

Although combining V_p and attenuation measurements seems to be a promising approach, several limitations must be considered which may introduce practical difficulties. First and foremost, the assumption that CO_2 will occupy purely spherical patches of a single radius seems extraordinarily unlikely; a more feasible scenario might include lenticular CO_2 patches with a distribution of characteristic length scales and aspect ratios. Unfortunately, no analytic model exists which can explicitly accommodate this class of shapes. A distribution of length scales would likely flatten the attenuation curves visible in panel B of Figure D4 leading to a greater uncertainty in saturation estimates. Additionally, the WDO formulation, like most patchy saturation models, has not been rigorously tested on the lab scale due to difficulty in quantifying $\boldsymbol{r}$ in core samples. Finally, quantitative tomographic estimation of P-wave attenuation is non-trivial although preliminary analysis of the Frio II CASSM datasets using the centroid shift method (Quan and Harris, 1997) suggests that such effects should be observable.

6. Summary

Data collected by LBNL during the injection phase of the Frio-II brine pilot from seismic monitoring, geochemical sampling, and the flow and transport modeling have been summarized in this report. The results include demonstration of the new seismic monitoring methodology incorporated in a unique instrumentation deployment with the recently developed U-tube geochemical sampling methodology. The geochemical sampling included aqueous chemistry (pH, EC, Eh) and organic and metal analysis as well as gaseous analysis. Gas analysis included CO_2 concentration (showing breakthrough in the monitoring well), tracers (PFTs, KR and SF_6, Xe and Kr) in addition to the unique use of CD_4 as a tracer. Both seismic and sampling data sets can be used to provide fundamental input and constraints to flow and transport modeling. Modifications to the Frio flow model, using seismic monitoring as a constraint, are being incorporated in a methodology aimed at iterative inversion. Additionally, recent work developing the petrophysical relationships governing the seismic response demonstrates the sensitivity of seismic monitoring in a brine aquifer, including the possibility of joint analysis of attenuation and velocity to improve saturation estimates. This work represents the foundation for continuing analysis of the highly successful Frio pilot project results within the GEOSEQ project at LBNL.

References:

Altunin, V.V., Thermophysical Properties of Carbon Dioxide, 1975 Publishing House of Standards, p. 551 (in Russian).

Batzle, M., and Z. Wang, Seismic Properties Of Pore Fluids, 1992, *Geophysics*, *57*, No.11, p. 1396-1408

Brie, A., F. Pampuri, A.F. Marsala, and O. Meazza, Shear sonic intepretation in gas-bearing sands, 1995, SPE Annual Technical Conference and Exhibition, p. 701-710

Carcione, J.M., S. Picotti, D. Gei and G. Rossi, Physics and Seismic Modeling for Monitoring CO_2 Storage, 2006, Pure and Applied Geophysics, Vol. 163, p.175-207.

Daley, T.M., R.D. Solbau, J.B. Ajo-Franklin, S.M. Benson, 2007, Continuous active-source monitoring of CO_2 injection in a brine aquifer, Geophysics, v72, n5, pA57–A61, DOI:10.1190/1.2754716.

Daley, T.M., Myer, L.R., Peterson, J.E., Majer, E.L., Hoversten, G.M., 2007, Time-lapse crosswell seismic and VSP monitoring of injected CO_2 in a brine aquifer, Environmental Geology, DOI 10.1007/s00254-007-0943-z.

Doughty C, Freifeld BM, Trautz RC (2007) Site characterization for CO_2 geologic storage and vice versa: the Frio brine pilot, Texas, USA as a case study. Environmental Geology, DOI 10.1007/s00254-007-0942-0.

Dutta, N.C., and A.J. Seriff, On White's model of attenuation in rocks with partial gas saturation, 1979, Geophysics, Vol. 44, p. 1806-1812

Freifeld, B.M., Trautz, R.C., Yousif K.K., Phelps, T.J., Myer, L.R., Hovorka, S.D., and Collins, D., The U-Tube: A novel system for acquiring borehole fluid samples from a deep geologic CO_2 sequestration experiment, J. Geophys. Res., 110, B10203, doi:10.1029/2005JB003735, 2005.

Freifeld, B. M. & Trautz, R. C., 2006, Real-time quadrupole mass spectrometer analysis of gas in borehole fluid samples acquired using the U-tube sampling methodology. Geofluids 6 (3), 217–224. doi:10.1111/j.1468-8123.2006.00138.x,

Kharaka, Y.K., J.J. Thordsen, D.R. Cole, S.D. Hovorka, and T. D. Bullen, Potential environmental issues of CO_2 storage in saline aquifers: Geochemical results from the Frio Brine Pilot tests, Texas, USA, Goldschmidt Conference in Cologne, Germany, 19-24 August, 2007.

Lemmon, E.W., M.O. McLinden, and D.G. Friend, Thermophysical Properties of Fluid Systems, 2005, NIST Chemistry Web Book, NIST Standard Reference Data base Number 69 , National Institute of Standards and Technology, ed. P.J. Linstrom and W.G. Mallard

Mroz E.J., Alei M., Cappis J.H., Guthals P.R, Mason A.S. and Rokop D.J. (1989a) Detection of multiply deuterated methane in the atmosphere. Geophysical Research Letters, 16, 677-678.

Mroz E.J., Alei M., Cappis J.H., Guthals P.R., Mason A.S. and Rokop D.J. (1989b) Antarctic atmospheric tracer experiments. Journal of Geophysical Research Letters, 94, 8577-8583.

Quan, Y.,and J.M. Harris, Seismic attenuation tomography using the frequency shift method, 1997, Geophysics, Vol. 62, No. 3, p. 895-905

Wang, Z. and A.M. Nur, Effects of CO_2 Flooding on Wave Velocities in Rocks With Hydrocarbons, 1989, SPE Reservoir Engineering, Vol. 4, No. 4, p. 429-436

Wang, Z., M.E. Cates and R.T. Langan, Seismic monitoring of a CO_2 flood in a carbonate reservoir: A rock physics study, 1998, Geophysics, Vol. 63, No. 5, p. 1604-1617.

White, J.E., Computed seismic speeds and attenuation in rocks with partial gas saturation, 1975, Geophysics, Vol. 40, p. 224-232

Acknowledgements:
This work was supported by the GEOSEQ project for the Assistant Secretary for Fossil Energy, Office of Coal and Power Systems through the National Energy Technology Laboratory, of the U.S. Department of Energy, under contract No. DE-AC02-05CH11231. Thanks to Susan Hovorka of Univ. of Texas, Bureau of Economic Geology for management of the Frio project, and to Dan Collins and David Freeman of Sandia Technologies for field support duing Frio II. Thanks to Don Fussell of VCable LLC and Ernie Majer and Ray Solbau of LBNL for discussions and advice, and to Fenglin Niu of Rice Univ. for field support, and to Paul Silver of the Carnegie Institution for work on continuous monitoring.

Appendix A. CASSM delay-time data.

Figure A1 is a summary of key data. The following figures are individual sensor data plots. Note that all data plots are updated versions of those used in Daley et al. (2007).

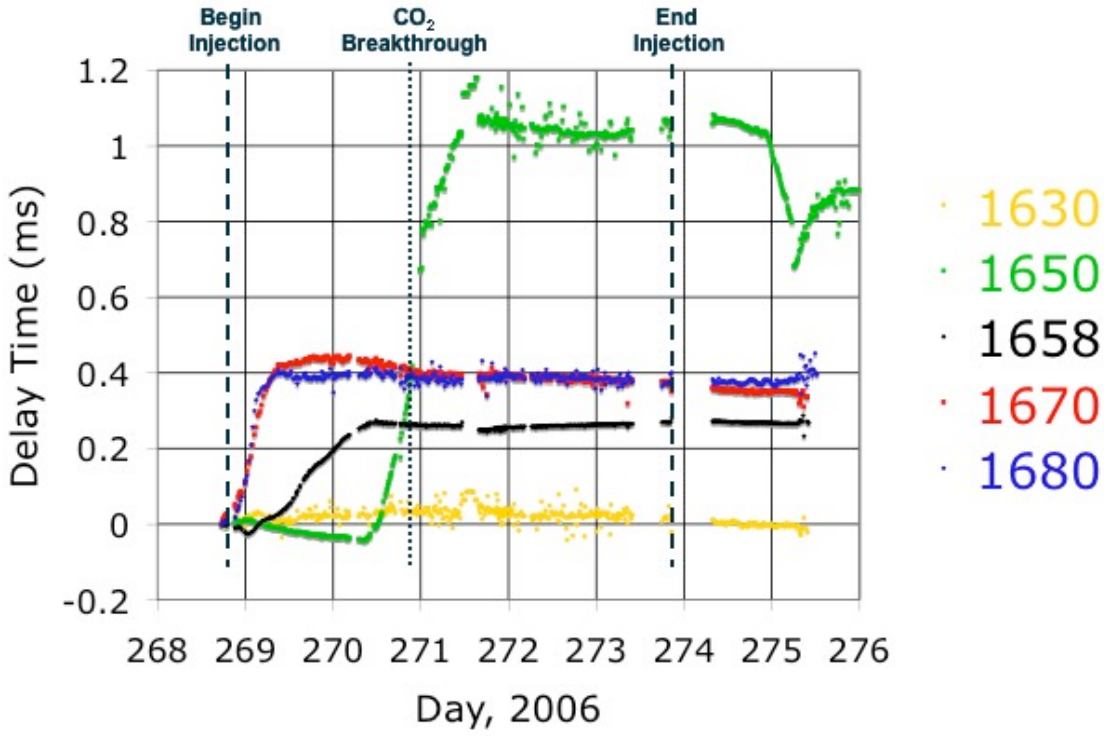

Figure A1. Delay time measurements for five sensor depths (m). Change in delay time is assumed to be caused by the change in CO_2 saturation and/or plume thickness. No change is seen at the shallowest control depth (1630 m) whereas the other depths show progressively later increase in delay time with decreasing depth, thereby monitoring the upward movement of the CO_2 plume.

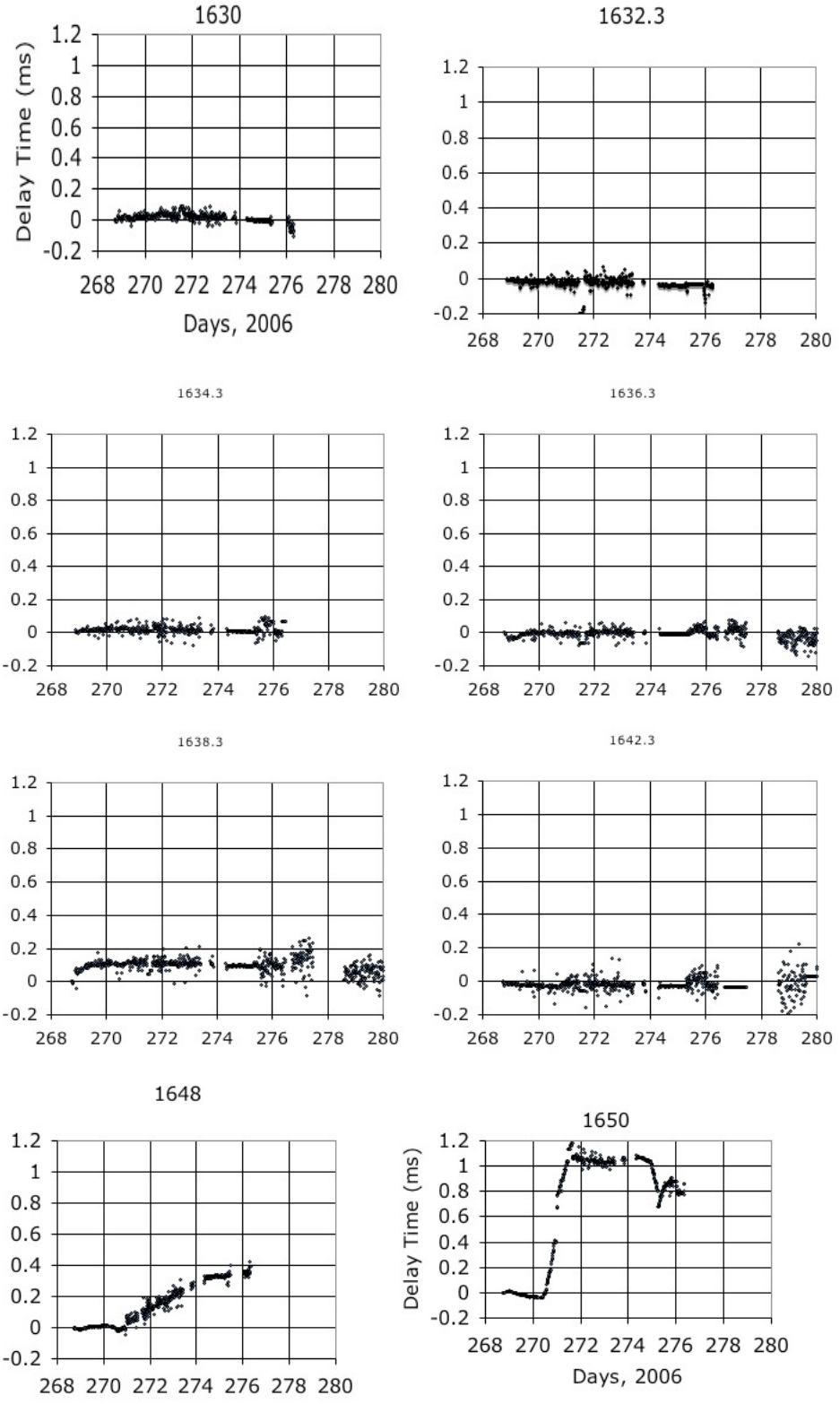
1630
1632.3
1634.3
1636.3
1638.3
1642.3
1648
1650
Delay Time (ms)
Days, 2006
1.2
1
0.8
0.6
0.4
0.2
0
-0.2
268 270 272 274 276 278 280

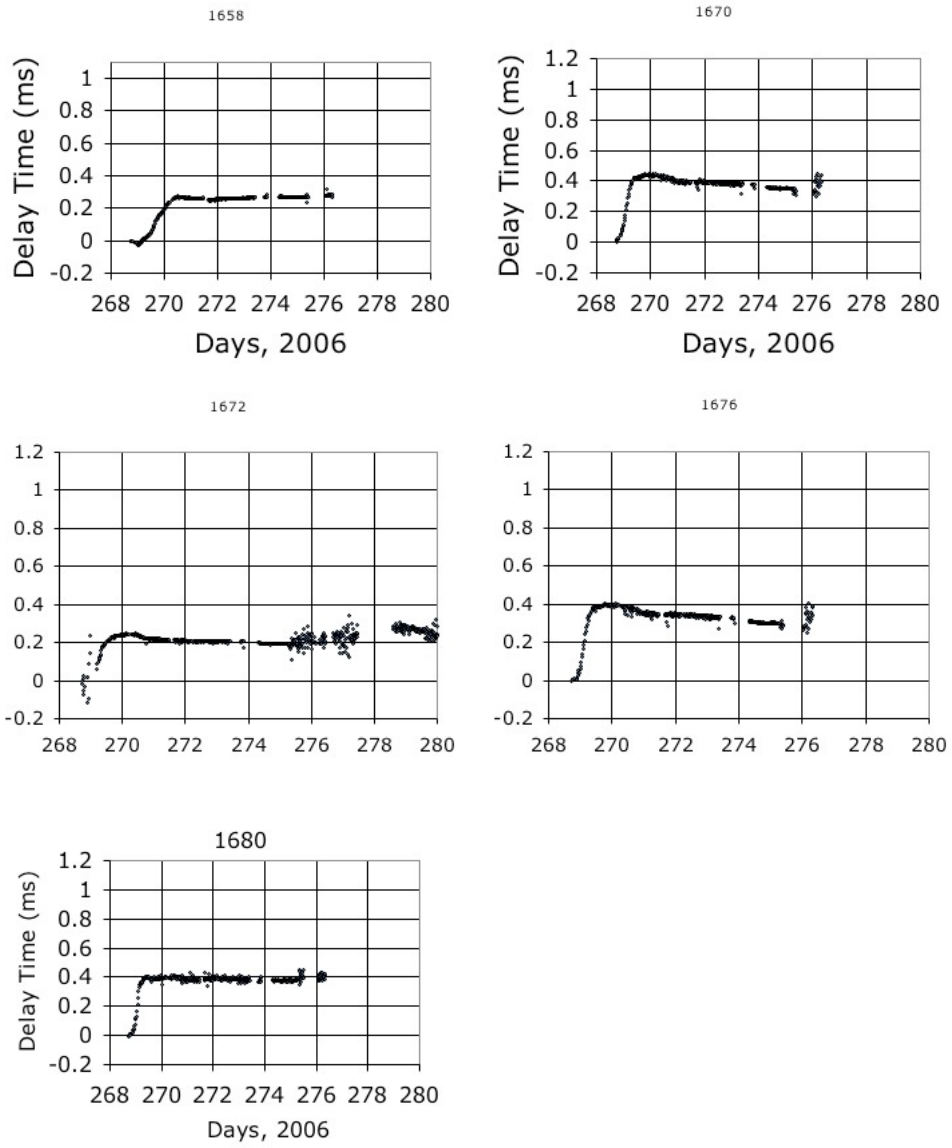

Figures A2. Plots of delay time (change in seismic crosswell travel time), in milliseconds, for the CASSM experiment over about 8 days in 2006. Depth of sensor in meters is label at top of each plot. The response for each sensor is affected by heterogeneity along the source-sensor raypath with the amount of delay time observed being affected by CO_2 saturation and thickness of the CO_2 plume along a raypath. Nonetheless, sensors above the reservoir (1630-1642 m) have essentially no change, while the top reservoir sensors (1648 and 1650 m) have later and larger change, and deeper sensors have earlier change. Notable events, as shown in Figure A1, are beginning injection at day 268.8, observed breakthrough (via U-tube sample) at day 270.9, and end of injection at day 273.8.

Appendix B. Hydrologic and Geochemical Data

Table B1. Samples Collected During the Frio II Experiment

U-tube notes from LBNL (11/14/06) nr - not recorded

Well	USGS water sample (06FCO2-)	USGS inline pH-T-EC?	Date	start purge cycle	Sample Collected U-tube Fill	Dump cycle Open M44	USGS sample	ORNL sample	Fluorescein sample	Close M44	Gas MS sample	Gas Dmethane sample	End Cycle
obs	303	yes	9/25/2006	10:05	9/25/06 9:08	nr	10:35	10:35	10:40	nr	11:05	11:11	
obs	none	yes	9/25/2006	11:13	9/25/06 11:13	nr	no sample	no samples	no samples	nr			
obs	304	yes	9/25/2006	14:34	9/25/06 12:17	nr	15:04			nr	15:22		
obs	305	yes	9/25/2006	15:28	9/25/06 15:28	nr	15:52	nr	nr	nr			
obs	306	yes	9/25/2006	nr	9/25/06 16:16		21:11		21:15				
obs	307	yes	9/26/2006	7:01	9/25/06 21:48	nr	7:27	7:32	7:30	8:05			
obs	308	yes	9/26/2006	9:18	9/26/06 7:49	***nr***	9:44	9:49	9:49		10:02	no	10:45
obs	309	yes	9/26/2006	12:48	9/26/06 10:07	***nr***	13:16	13:18	13:17	13:20	13:37	no	13:39
obs	310	yes	9/26/2006	13:39	9/26/06 13:40	14:01	14:07	14:08	14:08	14:11	14:25		14:29
obs	311	yes	9/26/2006	16:29	9/26/06 14:26	16:53	16:58	16:59	16:58	17:01	17:17	no	17:21
obs	312	yes	9/26/2006	18:41	9/26/06 17:19	19:02	19:08	19:10	19:08	19:13	19:29	no	19:33
obs	313	yes	9/26/2006	19:55	9/26/06 19:31	nr	20:20	nr	nr	nr	nr		
obs	314	yes	9/26/2006	22:20	9/26/06 20:43	nr	22:42	nr	nr	nr	nr		
obs	315	yes	9/27/2006	0:35	9/26/06 23:03	nr	1:02	nr	nr	nr	nr		
obs	316	yes	9/27/2006	2:55	9/27/06 1:24	nr	3:23	nr	nr	nr	nr		
obs	317	yes	9/27/2006	5:23	9/27/06 3:53	5:45	5:50	5:52	5:52	5:55	6:18	no	6:21
obs	318	yes	9/27/2006	7:51	9/27/06 6:20	8:12	8:18	8:21	8:19	8:23	8:39	no	8:42
obs	319	yes	9/27/2006	10:12	9/27/06 8:40	10:33	10:39	10:41	10:40	10:44	11:01	no	11:05
obs	320	yes	9/27/2006	12:35	9/27/06 11:05	12:56	13:02	13:05	13:03	13:07	13:27	no	13:30
obs	321	yes	9/27/2006	15:01	9/27/06 13:31	15:22	15:27	15:30	15:28	15:32	15:33	no	15:55
obs	322	yes	9/27/2006	17:26	9/27/06 15:56	17:47	17:53	17:56	17:54	17:58	18:18	no	18:22
obs	323	yes	9/27/2006	19:52	9/27/06 18:22	20:13	20:19	20:21	20:20	20:24	20:39	no	20:58
obs	324	yes	9/27/2006	22:12	9/27/06 20:42	22:23	22:40	22:42	22:41	22:44	22:59	no	23:03
obs	325	yes	9/27/2006	23:32	9/27/06 23:02	23:53	23:59	0:02	0:00	0:04	0:20	no	0:22
obs	326	yes	9/28/2006	0:37	9/28/06 0:22	0:58	1:04	1:06	1:05	1:09	1:25	no	1:27
obs	327	yes	9/28/2006	1:43	9/28/06 1:27	2:04	2:10	2:10	2:10	2:14	2:56	no	*2:58*
obs	328	yes	9/28/2006	3:14	9/28/06 2:58	3:35	3:41	3:43	3:43	3:46	4:04	no	4:06
obs	329	yes	9/28/2006	4:21	9/28/06 4:06	4:42	4:49	4:50	4:49	4:53	5:08	5:08	nr
obs	330	yes	9/28/2006	5:29	9/28/06 5:14	5:50	5:56	5:58	5:58	6:00	6:16	6:17	6:22
obs	331	yes	9/28/2006	*6:44*	9/28/06 6:22	6:59	7:05	7:07	7:06	7:10	7:34	7:34	7:38
obs	none	yes	9/28/2006	7:55	9/28/06 7:38	8:11	no sample	8:24	8:23	8:26	8:30	8:46	8:46
obs	332	yes	9/28/2006	9:01	9/28/06 8:46	9:23	9:29	9:31	9:33	9:33	9:48	9:54	9:54
obs	none	yes	9/28/2006	10:11	9/28/06 9:56	10:32	no sample	10:40	no samples	10:43	10:59	11:04	11:06
obs	333	yes	9/28/2006	11:21	9/28/06 11:06	11:42	11:49	11:52	11:48	11:53	12:10	12:17	12:19
obs	none	yes	9/28/2006	12:34	9/28/06 12:19	12:55	no sample	13:03	13:05	13:06	13:39	13:48	13:48
obs	334	yes	9/28/2006	14:04	9/28/06 13:49	14:25	14:34	14:35	14:36	14:37	14:59	15:08	nr
obs	335	yes	9/28/2006	15:12	9/28/06 15:09	15:50	15:55	15:59	no samples	16:01	16:23	16:32	16:35
obs	336	yes	9/28/2006	*16:48*	9/28/06 16:33	17:09	17:18	17:18	17:18	17:20	17:34	17:46	17:48
obs	none	yes	9/28/2006	18:04	9/28/06 17:49	18:25	no sample	18:34	no samples	18:36	19:10	19:19	19:19
obs	337	yes	9/28/2006	19:34	9/28/06 19:19	19:55	20:02	20:04	20:02	20:06	20:22	20:29	20:29
obs	none	yes	9/28/2006	20:45	9/28/06 20:30	21:06	no sample	21:15	no samples	21:17	21:31	21:38	21:38
obs	338	yes	9/28/2006	21:55	9/28/06 21:40	22:16	22:23	22:25	22:23	22:28	22:47	22:54	22:54
obs	none	yes	9/28/2006	23:10	9/28/06 22:55	23:31	no sample	23:40	no samples	23:42	23:57	0:05	0:05
obs	339	yes	9/29/2006	0:20	9/29/06 0:05	0:42	0:48	0:51	0:48	0:53	1:08	1:15	1:15
obs	340	yes	9/29/2006	1:30	9/29/06 1:15	1:51	1:58	1:58	1:58	2:00	2:02	2:16	2:25
obs	none	yes	9/29/2006	2:41	9/29/06 2:26	3:02	no sample	3:10	no samples	3:13	3:28	3:35	3:35
obs	341	yes	9/29/2006	3:51	9/29/06 3:36	4:12	4:19	4:21	4:18	4:23	4:39	4:48	4:49
obs	342	yes	9/29/2006	5:04	9/29/06 4:49	5:26	5:33	5:35	5:33	5:37	5:58	6:04	6:05
obs	343	yes	9/29/2006	6:21	9/29/06 6:06	6:41	6:47	6:50	6:49	6:53	7:10	7:21	7:21
obs	none	yes	9/29/2006	7:36	9/29/06 7:22	7:57	no sample	8:07	8:01	8:08	8:32	8:37	8:38
obs	344	yes	9/29/2006	8:53	9/29/06 8:39	9:15	9:21	9:23	9:22	9:25	9:47	9:55	9:56
obs	345	yes	9/29/2006	10:11	9/29/06 9:56	10:32	10:39	10:40	10:38	10:43	11:02	11:09	11:11
obs	none	no	9/29/2006	11:26	nr	na	na	na	na	na	na	na	na
obs	346	yes	9/29/2006	12:29	9/29/06 11:11	12:49	12:57	12:59	12:58	13:01	13:23	13:27	13:28
obs	347	yes	9/29/2006	13:42	9/29/06 13:28	14:05	14:12	14:13	14:12	14:16	14:32	14:38	14:40
obs	348	yes	9/29/2006	14:55	9/29/06 14:40	15:16	15:24	15:25	15:24	15:27	15:43	15:48	15:49
obs	349	yes	9/29/2006	16:04	9/29/06 15:50	16:25	16:34	16:34	16:34	16:37	16:58	17:04	17:05
obs	350	yes	9/29/2006	17:20	9/29/06 17:05	17:41	17:47	17:50	17:47	17:52	18:08	18:14	18:15
obs	351	yes	9/29/2006	18:31	9/29/06 18:15	18:52	18:59	19:01	18:59	19:03	19:25	19:26	19:25

obs	none	yes	9/29/2006	19:40	9/29/06 19:25	20:01	no sample		20:10	20:10	20:13	20:28	20:34	20:35
obs	352	yes	9/29/2006	20:50	9/29/06 20:35	21:11	21:19		21:20	21:18	21:22	21:36	21:41	21:41
obs	none	yes	9/29/2006	21:56	9/29/06 21:41	22:17	no sample		22:27	22:27	22:28	22:44	22:49	22:49
obs	353	yes	9/29/2006	23:04	9/29/06 22:49	23:24	23:33		23:34	23:33	23:36	23:50	23:55	23:55
obs	none	yes	9/30/2006	0:10	9/29/06 23:56	0:31	no sample		0:40	0:38	0:42	0:56	1:02	1:02
obs	none	yes	9/30/2006	1:17	9/30/06 1:02	1:39	no sample		1:47	1:46	1:50	2:03	2:09	2:10
obs	354	yes	9/30/2006	2:25	9/30/06 2:10	2:46	2:54		2:55	2:54	2:57	3:25	3:32	3:33
obs	none	yes	9/30/2006	3:48	9/30/06 3:34	4:10	no sample		4:18	no samples	4:21	4:37	4:44	4:45
obs	none	yes	9/30/2006	5:00	9/30/06 4:45	5:21	no sample		5:29	5:28	5:32	6:18	6:25	6:26
obs	355	yes	9/30/2006	*6:38*	9/30/06 6:23	*7:04*	*7:10*		*7:11*	*7:10*	*7:13*	*8:14*	*8:21*	*8:24*
obs	none	yes	9/30/2006	9:22	9/30/06 9:07	9:44	no sample		9:52	9:49	9:55	10:10	10:16	10:17
obs	356	yes	9/30/2006	10:32	9/30/06 10:17	nr ?	11:01		11:02	11:02	11:04	11:23	11:29	11:30
obs	none	yes	9/30/2006	11:45	9/30/06 11:31	12:07	no sample		12:17	12:11	12:18	12:34	12:39	12:41
obs	none	yes	9/30/2006	12:56	9/30/06 12:41	13:11	no sample		13:19	13:19	13:22	13:38	13:46	13:47
obs	357	yes	9/30/2006	14:12	9/30/06 13:48	14:27	14:32		14:35	14:32	14:38	15:15	15:23	15:24
obs	358	yes	9/30/2006	19:10	9/30/06 15:24	19:25	19:36		19:36	19:35	19:36	19:50	19:55	19:55
obs	none	yes	9/30/2006	20:40	9/30/06 19:56	20:55	no sample		21:05	21:04	20:07	20:40	20:45	20:45
obs	none	yes	9/30/2006	22:30	9/30/06 21:46	22:46	no sample	no samples		22:52	22:57	23:23	23:28	23:29
obs	359	yes	10/1/2006	0:14	9/30/06 23:30	0:29	0:37	no samples		0:35	0:40	0:56	1:01	1:01
obs	none	yes	10/1/2006	2:17	10/1/06 1:02	2:32	no sample		2:41	2:39	2:43	3:03	3:09	3:10
obs	none	yes	10/1/2006	6:36	10/1/06 3:10	6:52	no sample		7:01	6:56	7:03	7:42	7:49	*7:49*
obs	none	yes	10/2/2006	12:32		12:47	no sample		12:58	nr	13:01	13:23	13:23	13:26
obs	362	yes	10/2/2006	17:46		17:46	17:54		17:56	17:54	17:57	18:11	18:16	18:17
obs	none	yes	10/2/2006	21:23		21:53	no sample		22:01	21:55	22:04	22:18	22:24	22:25

Injection Well

Injection	360		10/1/2006	5:38	5:55	6:04		6:01	6:02	6:05	6:19	6:26	6:28
Injection	361		10/1/2006	14:00	14:24	*14:30*		*14:30*	*14:30*	nr	nr	nr	nr
Injection	none		10/2/2006	11:36	11:36	no sample	???		???	nr	???	???	11:50
Injection	none		10/2/2006	14:41	14:56	no sample		15:24	nr	15:24	15:36	nr	nr
Injection	none		10/2/2006	16:09	16:24	no sample		16:33	16:33	16:35	16:52	16:57	16:58
Injection	363		10/2/2006	19:44	20:14	20:23		20:24	20:23	20:25	21:05	21:13	21:15

END OF USEFUL IN-LINE pH-T-EC RESULTS

Injection	none		10/3/2006	0:26	0:26	aborted	aborted	aborted	nr	aborted	aborted	nr
Injection	none		10/3/2006	1:26	1:55	aborted	aborted	aborted	nr	aborted	aborted	nr
obs	none	no	10/3/2006	2:15	2:43	aborted	aborted	aborted	nr	aborted	aborted	nr

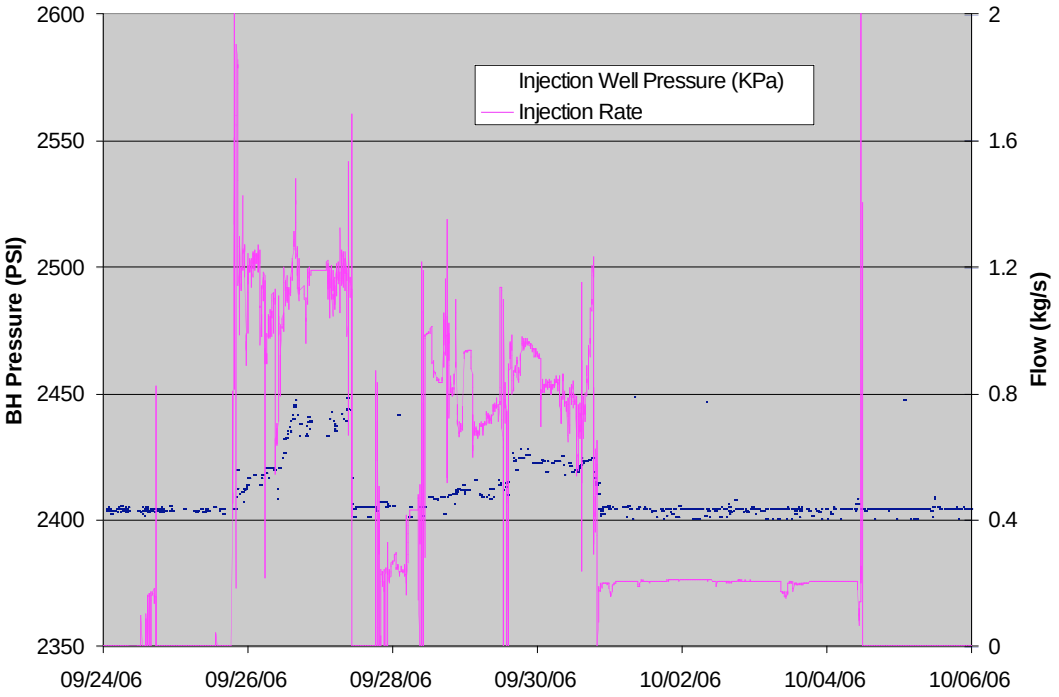

Figure B1. CO_2 injection mass flow rate and bottomhole pressure in the injection well. Note that the noisy signal for the injection well pressure is caused by electrical interference between the tubing-deployed seismic source and the downhole pressure gage.

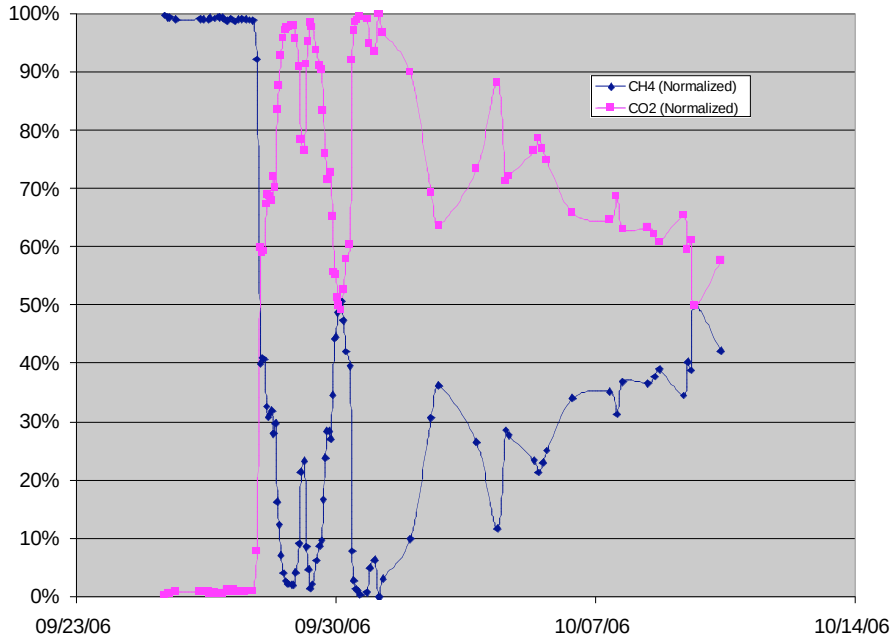

Figure B2. Percentages of CO_2 and CH_4, normalized to 1. Initial breakthrough of CO_2 occurred in the sample collected 50 hours 12 minutes after initial CO_2 injection.

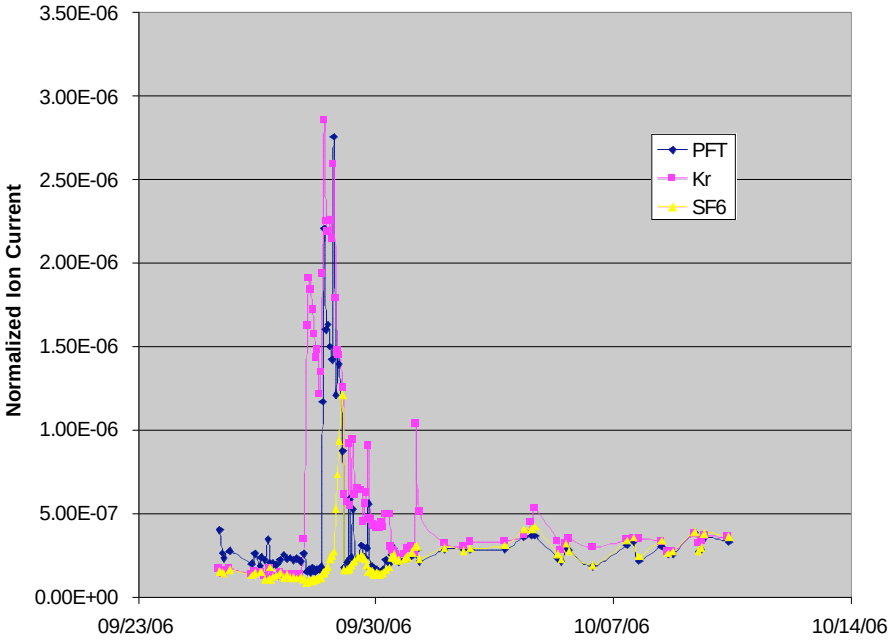

Figure B3. Qualitative breakthrough curves for perfluorocarbon, krypton, and SF6 as analyzed on the field quadrupole mass spectrometer. Note that the Kr breakthrough curve occurs at the same time as the CO_2 breakthrough, although it was injected 16 hours later.

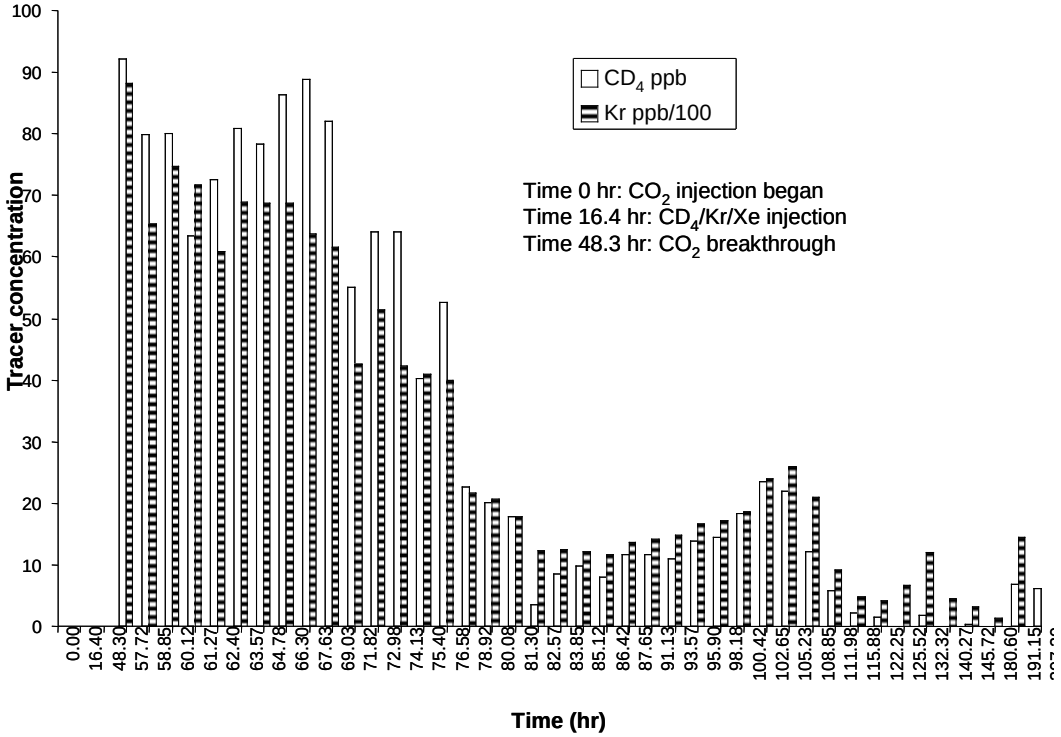

Figure B4. Krypton and CD_4 tracer test results courtesy of the Jim Underschultz and Chris Boreham, CO2CRC, Auastralia. CD_4 concentration (ppb) from m/z 20.06 and Kr concentration (ppb/100) from m/z 83.91 normalised to [CO_2]. Note: [Kr] in 'air' is 1140 ppb with nominal mass 84 isotope abundance of 56.9%, therefore [^{84}Kr/100] in 'air' is 6.49 on the tracer concentration axis.

Table B2. Chemical analysis of U-tube samples. Analysis provided by Y. Kharaka and J. Thordsen USGS, Menlo Park.

SAMPLE	DATE		site	field EC uS/cm	pH	T °C	MS Q Li 7 mg/L	MS Q Na 23 mg/L	MS Q K 39 mg/L	ise NH4+ mg/L	MS Q Mg 24 mg/L	MS Q Ca 43 mg/L	MS Q Sr 88 mg/L	MS Q Ba 138 mg/L	MS Q Mn 55 mg/L	MS Q Fe 54 mg/L
06FCO2-211	9/6/06	14:00	observation well-	131600	7.2	33	3.2	35621	213	52	337	2646	104	62	4.3	31
06FCO2-212	9/6/06	16:55	observation well-	133000	6.7	25	4.7	35618	209		343	2606	103	62	4.3	17
06FCO2-213	9/6/06	17:55	observation well-	131100	6.7	29	4.3	35545	205	52	331	2607	102	62	4.3	26
06FCO2-232	9/10/06	11:00	injection well-surf	132100	7.3	33	3.5	36325	210	52	334	2652	105	63	4.1	27
06FCO2-233	9/10/06	11:45	injection well-lg K	130900	*6.2*	29	4.0	34568	209	52	319	2604	102	61	4.1	23
06FCO2-234	9/10/06	12:30	injection well-sm	131500	6.8	28	4.2	35788	211		326	2613	103	62	4.1	24
06FCO2-238	9/11/06	10:30	injection well-lg K	126800	*6.3*	35	3.6	34625	201	51	315	2516	99	59	4.0	21
06FCO2-301	9/21/06	14:00	frac tank	135200	6.6	25	3.3	36797	210		326	2602	104	61	4.1	*2.3*
06FCO2-302	9/25/06	8:38	observation well -	128700	7.1	20	2.8	35011	181	42	263	2137	83	33	4.0	22
06FCO2-306	9/25/06	21:11	observation well -	127700	6.7	24	2.9	34470	184	43	263	2176	85	36	4.3	26
06FCO2-307	9/26/06	7:28	observation well -	129100	6.9	21	3.0	34106	187	43	279	2206	87	39	4.5	32
06FCO2-309	9/26/06	13:15	observation well -	129200	6.8	25	2.9	34127	186	44	286	2250	88	43	4.6	35
06FCO2-311	9/26/06	16:58	observation well -	129700	6.8	26	3.0	34435	192		300	2296	90	45	4.7	38
06FCO2-313	9/26/06	20:20	observation well -	131600	6.8	23	3.1	34387	195		308	2349	92	48	4.7	37
06FCO2-315	9/27/06	1:02	observation well -	130700	6.8	24	3.2	34050	192	47	307	2357	92	50	4.7	41
06FCO2-317	9/27/06	5:50	observation well -	132400	6.6	23	3.1	34222	199		311	2414	94	53	4.6	36
06FCO2-319	9/27/06	10:38	observation well -	131100	6.6	25	3.2	35688	198		320	2439	96	55	4.5	35
06FCO2-321	9/27/06	15:27	observation well -	130300	6.6	28	3.1	34463	197	46	306	2360	93	50	4.4	31
06FCO2-323	9/27/06	20:18	observation well -	128100	6.5	25	2.9	33999	187		273	2204	85	33	3.8	21
06FCO2-324	9/27/06	22:40	observation well -	128800	6.0	24	2.9	34267	188	41	278	2221	86	35	4.1	42
06FCO2-325	9/28/06	0:00	observation well -	129000	5.6	25	3.0	34846	193	26	298	2420	92	47	5.5	136
06FCO2-326	9/28/06	1:04	observation well -	128100	5.9	25	3.0	33913	192	41	295	2382	90	44	6.2	235
06FCO2-327	9/28/06	2:10	observation well -	130100	5.7	24	3.0	34524	194	38	298	2394	91	45	6.7	267
06FCO2-328	9/28/06	3:41	observation well -	129300	5.7	24	2.9	34784	194	36	297	2374	91	43	7.3	313
06FCO2-329	9/28/06	4:48	observation well -	128600	5.7	24	3.0	34409	188	28	296	2347	90	42	7.7	333
06FCO2-330	9/28/06	5:56	observation well -	128200	5.8	24	2.9	34128	193	32	299	2406	90	43	8.1	371
06FCO2-331	9/28/06	7:05	observation well -	128500	5.8	23	3.0	34689	192	30	294	2374	91	43	8.5	395
06FCO2-332	9/28/06	9:28	observation well -	128900	5.8	24	3.0	35137	185	31	296	2340	89	41	8.4	369
06FCO2-333	9/28/06	11:48	observation well -	127800	5.6	24	3.1	35449	190	40	299	2357	90	42	8.3	332
06FCO2-334	9/28/06	14:32	observation well -	129800	5.5	22	3.0	35389	194	25	298	2366	90	43	7.7	241
06FCO2-335	9/28/06	15:56	observation well -	130800	5.5	26	3.1	35299	191	25	303	2360	91	44	7.2	202
06FCO2-336	9/28/06	17:15	observation well -	131500	5.6	24	3.0	35577	190	36	299	2357	90	43	8.4	380
06FCO2-337	9/28/06	20:02	observation well -	130400	5.7	21	2.9	34145	182	33	281	2314	89	36	8.6	449
06FCO2-338	9/28/06	22:23	observation well -	132600	5.8	20	2.9	35002	182	39	277	2319	88	19	9.6	552
06FCO2-339	9/29/06	0:48	observation well -	136400	5.9	19	2.8	37706	174		269	2262	83	17	11.3	726
06FCO2-340	9/29/06	1:58	observation well -	131900	5.8	23	2.8	34731	182	38	277	2345	88	27	8.4	375
06FCO2-341	9/29/06	4:18	observation well -	126400	6.1	21	2.9	33032	184		296	2502	91	49	12.6	861
06FCO2-343	9/29/06	6:47	observation well -	126200	6.1	21	3.1	32632	190		284	2403	93	54	14.2	1013
06FCO2-344	9/29/06	9:22	observation well -	127000	6.0	23	3.0	33424	196		291	2417	94	52	10.1	592
06FCO2-345	9/29/06	10:38	observation well -	126700	5.9	24	3.0	34381	195		292	2381	93	52	9.8	551
06FCO2-346	9/29/06	12:56	observation well -	128800	5.8	25	3.0	34409	195		296	2425	94	53	8.4	365
06FCO2-347	9/29/06	14:10	observation well -	127600	5.9	26	3.3	33699	197		294	2398	94	52	9.1	507
06FCO2-348	9/29/06	15:23	observation well -	129500	5.7	25	3.0	35383	199		306	2424	96	53	7.5	254
06FCO2-349	9/29/06	16:32	observation well -	128400	5.8	25	3.2	34043	200		304	2446	94	53	8.2	385
06FCO2-350	9/29/06	17:47	observation well -	128900	5.8	24	3.0	35097	194		290	2385	93	53	8.5	412
06FCO2-351	9/29/06	18:58	observation well -	130700	5.7	24	3.2	34774	198	36	301	2461	96	54	7.3	239
06FCO2-352	9/29/06	21:11	observation well -	131200	5.6	23	3.1	34638	203		305	2481	97	56	7.2	228
06FCO2-353	9/29/06	23:30	observation well -	131100	5.6	23	3.2	35619	200	36	309	2440	96	55	7.2	240
06FCO2-354	9/30/06	2:54	observation well -	131500	5.6	23	3.3	35037	206	29	294	2493	97	57	7.2	192
06FCO2-355	9/30/06	7:10	observation well -	130500	5.7	23	3.1	35118	197	33	303	2377	94	52	8.4	410
06FCO2-356	9/30/06	11:00	observation well -	125400	6.0	25	3.2	34479	179	42	268	2155	84	43	9.3	832
06FCO2-357	9/30/06	14:32	observation well -	124700	6.1	27	2.8	32814	189		300	2259	90	46	12.5	1140
06FCO2-358	9/30/06	19:33	observation well -	125300	6.1	24	3.0	33520	191		305	2227	89	44	12.1	1170
06FCO2-359	10/1/06	0:29	observation well -	129100	6.0	23	2.9	33697	194		307	2247	87	37	11.2	820
06FCO2-360	10/1/06	6:05	injection well - U-	182300	5.9	23	5.3	56343	375	84	652	4425	177	105	27	910
06FCO2-361	10/2/06	15:20	injection well - U-	164500	6.1	24	4.4	47605	302	65	484	3735	138	89	25	292
06FCO2-362	10/2/06	17:53	observation well -	132400	5.9	24	2.9	35937	186	34	287	2394	93	39	9.8	150
06FCO2-363	10/2/06	20:22	injection well - U-	169400	5.8	24	4.3	50809	304	56	469	3654	142	98	24	98
06FCO2-370	10/9/06	11:00	observation well -	131300	*5.9*	25	2.9	34886	194		294	2415	94	47	7.4	204
06FCO2-371	10/9/06	13:10	observation well -	133800	*6.5*	24	3.1	36274	200		283	2293	88	31	2.2	*2.5*
06FCO2-372	10/9/06	13:15	observation well -	132900	*5.8*	26	3.2	36705	200	*44*	327	2495	97	56	8.0	143
06FCO2-373	10/9/06	15:10	observation well -	132300	*6.0*	25	3.0	35500	199		305	2447	98	50	6.4	63
06FCO2-374	10/9/06	17:00	observation well -	131400	*6.3*	27	2.9	34939	195		302	2321	89	40	3.7	12
06FCO2-375	10/10/06	9:56	observation well -	132600	*6.4*	21	3.0	34608	199		304	2401	93	38	2.4	*2.9*
06FCO2-376	10/10/06	10:00	injection well - lg	144000	*6.7*	21	4.0	37307	244		386	2971	109	62	24	76
06FCO2-381	11/2/06	15:15	observation well -	132500	*5.8*	19	3.0	35553	205		320	2601	100	64	10.9	234
07FCO2-101	3/20/07	13:00	Obs well U (1-flush)	132800	*6.5*	28										
07FCO2-102	3/20/07	15:28	Obs well U-tube	135000	6.2	26										
07FCO2-103	3/20/07	16:30	Obs well U-tube	136600	5.9	25										

	MS Q	MS Q	MS Q	MS Q	MS Q	IC	MS	IC	titr	titr	MS Q	MS Q	org	
SAMPLE	Zn 66	Co 59	Pb 208,(	Al 27	Cr 52	**Cl**	**Br**	**SO4**	**HCO3**	**H2S**	**SiO2**	**B 11**	**DOC**	**TDS**
	ug/L	*ug/L*	*ug/L*	*ug/L*	*ug/L*	mg/L	mg/L	mg/L	mg/L	mg/L	mg/L	mg/L	mg/L	mg/L
06FCO2-211	105	<5	*6*	<50	*107*	63336	75	2	175	<0.2	*34*	25	2.3	102838
06FCO2-212	669	<5	59	<50	*126*	62260	75		138		*26*	27		101618
06FCO2-213	940	<5	725	<50	*99*	61985	73	2	167	<0.2	*24*	25	4.1	101334
06FCO2-232	197	<5	<2.5	<50	*120*	63510	76	<0	152	<0.2	*29*	26	1.2	103689
06FCO2-233	390	<5	27	<50	*115*	62039	74	<0	*126*		*29*	26	2.5	100365
06FCO2-234	643	<5	121	<50	*114*	61914	74	<0	170		*31*	25	3.6	101470
06FCO2-238	397	<5	13	<50	*87*	60420	71	<0	*130*		*29*	25	2.3	98686
06FCO2-301	2449	<5	*6*	<50	*93*	62479	74		101		*21*	26		102930
06FCO2-302	8410	<5	<2.5	<50	*94*	58324	63		62		*12*	20	4.2	96354
06FCO2-306	9282	<5	<2.5	*101*	*94*	58520	64		60		*17*	21	3.8	96071
06FCO2-307	6468	<5	<2.5	<250	*57*	58763	64		70		*16*	21	3.7	96022
06FCO2-309	7097	<5	<2.5	<250	*82*	59424	66		76		*18*	22	4.6	96773
06FCO2-311	6966	<5	<2.5	<250	*70*	60122	67		81		*22*	23		97823
06FCO2-313	7323	*6*	<2.5	<250	*65*	60497	70		84		*21*	23		98227
06FCO2-315	6896	<5	<2.5	<250	*61*	60960	69		92		*20*	22	2.8	98410
06FCO2-317	6967	<5	<2.5	<250	*48*	61536	70		95		*21*	23		99190
06FCO2-319	7696	*14*	<2.5	<250	*48*	61270	72		101		*24*	23		100436
06FCO2-321	9080	<5	<2.5	<250	*49*	60752	69		89		*20*	23	2.7	98613
06FCO2-323	10066	<5	<2.5	<250	*49*	59206	65		44		*21*	21		96262
06FCO2-324	19324	<5	<2.5	<250	*56*	59190	66		153		*23*	21	4.0	96714
06FCO2-325	71066	*10*	*16*	<250	*53*	59796	71		649		*37*	23	5.6	98750
06FCO2-326	55731	*10*	62	<125	*69*	59478	69		1220		*46*	22	5.0	98141
06FCO2-327	71968	*14*	42	<125	*73*	59842	70		958		*62*	23	4.9	98923
06FCO2-328	69807	*14*	51	<125	*66*	59616	71		1053		*56*	22	4.5	99064
06FCO2-329	66062	*16*	49	<125	*60*	61391	70		1044		*58*	22	4.2	100434
06FCO2-330	66793	*14*	51	<125	*60*	59814	72		1132		*62*	23	3.9	98783
06FCO2-331	65717	*14*	59	<125	*58*	59576	71		1219		*60*	22	3.7	99172
06FCO2-332	52597	*11*	67	<125	*55*	60101	69		1171		*58*	22	3.5	100022
06FCO2-333	44967	*11*	192	<125	*64*	60404	69		1057		*55*	23	3.0	100524
06FCO2-334	39127	*11*	237	<125	*92*	60479	69		814		*50*	23	2.9	100196
06FCO2-335	41841	*15*	159	<125	*137*	60482	67		716		*50*	23	2.2	99969
06FCO2-336	34916	*18*	137	<125	*183*	60409	71		1091		*50*	21	2.9	100726
06FCO2-337	33204	*16*	106	<250	*170*	60303	77		1262		*45*	21	4.1	99346
06FCO2-338	31505	*11*	89	<250	*105*	61531	75		1701		*54*	20	4.6	101969
06FCO2-339	28953	*15*	86	<250	*77*	66262	73	66	2285		*61*	19	5.7	110111
06FCO2-340	30561	*12*	53	<250	*66*	62094	74	28	1265		*54*	20	4.2	101705
06FCO2-341	7783	*41*	65	<250	*48*	58707	74	17	2963		*63*	20	8.3	98968
06FCO2-343	6737	*25*	38	<250	*40*	58103	74	14	3255		*70*	18	6.1	98304
06FCO2-344	32257	*20*	107	<250	*36*	59651	75	15	2052		*66*	20	5.2	99055
06FCO2-345	23460	*17*	124	<250	*47*	59866	77	15	1943		*61*	21	4.3	100043
06FCO2-346	27344	*14*	122	<250	*39*	60515	74	15	1402		*59*	21	3.4	100033
06FCO2-347	20318	*16*	127	<250	*41*	59540	75	21	1768		*61*	22	3.4	98846
06FCO2-348	23606	*10*	137	<250	*39*	60983	75	12	1041		*52*	22	3.0	101015
06FCO2-349	22091	*14*	122	<50	*41*	60834	71	14	1371		*48*	22	3.5	100002
06FCO2-350	20389	*14*	124	<50	*62*	60776	75	15	1485		*46*	21	3.8	101053
06FCO2-351	22761	*8*	123	<50	*42*	61131	71	14	936		*41*	23	2.7	100491
06FCO2-352	23090	*8*	123	<50	*51*	61513	73	13	818		*42*	23	2.7	100612
06FCO2-353	21748	*8*	118	<50	*42*	61582	73	15	872		*49*	23	2.7	101727
06FCO2-354	22772	*7*	115	<50	*55*	61669	71	13	718		*42*	24	2.6	101066
06FCO2-355	18218	*10*	96	<50	*48*	61216	72	16	1309		*50*	22	2.9	101382
06FCO2-356	7519	*19*	59	<50	*34*	59033	66	24	2520		*67*	17	6.8	99902
06FCO2-357	3628	*29*	39	<50	*32*	58318	70	17	2867		*71*	19	8.8	98308
06FCO2-358	5039	*30*	38	<50	*28*	58167	69	13	2981		*66*	19	8.9	98969
06FCO2-359	10678	*25*	25	<50	*30*	59986	68	19	2278		*64*	22	5.8	99946
06FCO2-360	147158	*41*	1152	<250	*144*	95682	150	5	2761		*99*	53	7.3	162102
06FCO2-361	105137	<5	312	<250	*93*	81698	110	4	2591		*92*	42	7.6	137472
06FCO2-362	12190	*48*	*14*	<125	*69*	61629	74	27	822		*45*	27	2.7	101883
06FCO2-363	146183	<10	58	<250	*87*	84393	105	7	1445		*80*	47	8.4	141954
06FCO2-370	34508	*16*	*5*	<125	*54*	60921	85	14	*1275*		*55*	24		100628
06FCO2-371	1816	<5	<2.5	<125	*56*	62232	74	19	*50*		*9*	10		101617
06FCO2-372	11564	*6*	157	<125	*54*	62084	83	11	*561*		*43*	22	1.3	102989
06FCO2-373	27824	*22*	33	<125	*52*	61759	76	14	*171*		*47*	23		100872
06FCO2-374	2372	<5	<2.5	<125	*42*	61221	74	12	*32*		*8*	14		99333
06FCO2-375	1994	*7*	*3*	<125	*60*	61761	73	19	*163*		*8*	15		99759
06FCO2-376	34524	*10*	<2.5	<125	*51*	65358	86	2	*1592*		*48*	34		108462
06FCO2-381	6535	<5	*6*	<125	*45*	61737	84	7	*898*		*45*	24		102001

Appendix C. Flow Modeling Data Results

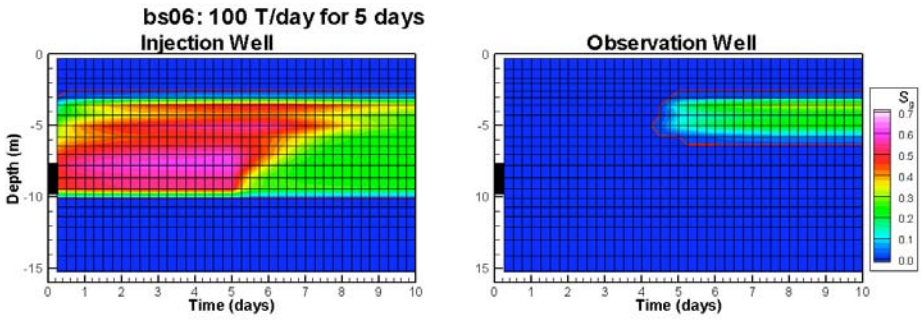

Figure C1. Example of initial flow modeling of the Frio II C-sand during injection.

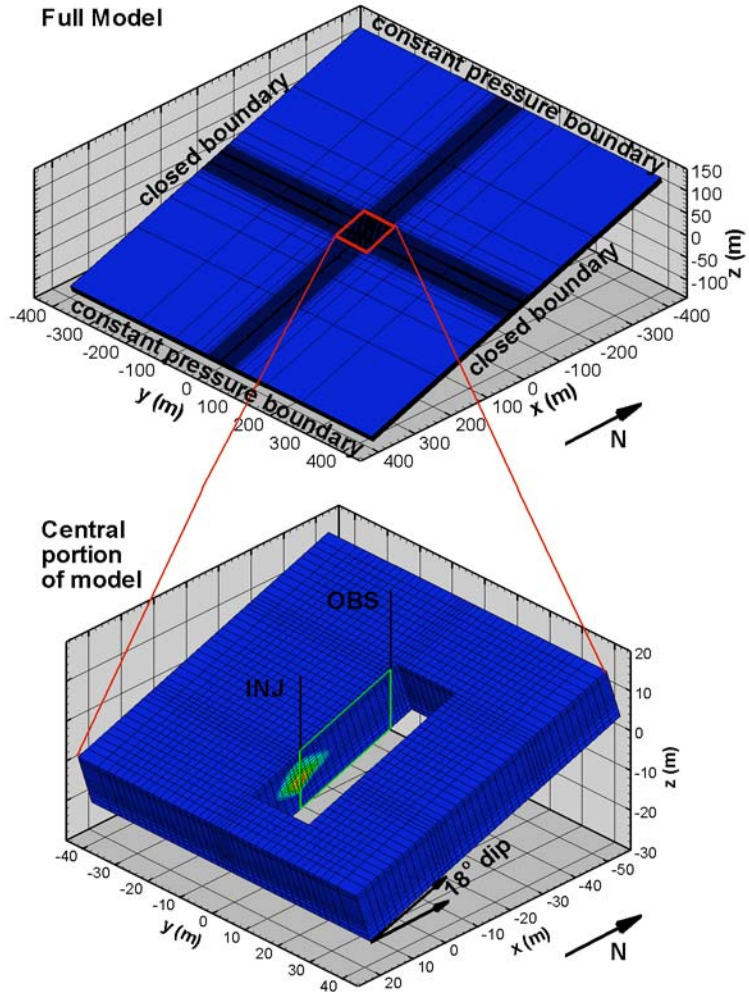

Figure C2 The revised TOUGH-2 model with a sample CO_2 plume after 10 hours of injection

Appendix D Petrophysical Modeling

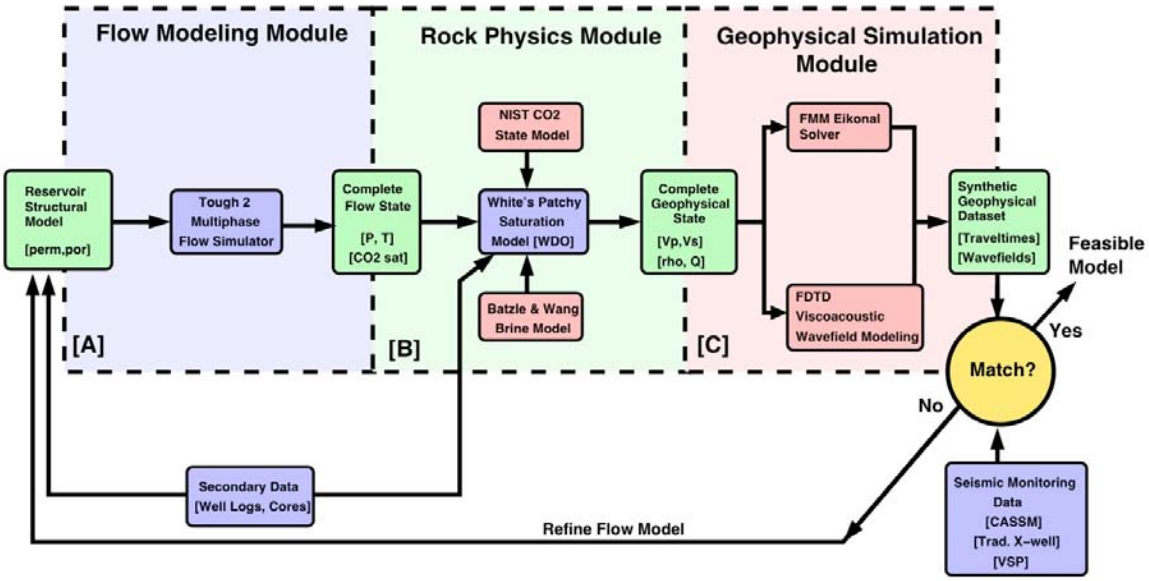

Figure D1. Block diagram of integration of flow modeling with geophysical monitoring via a rock physics model.

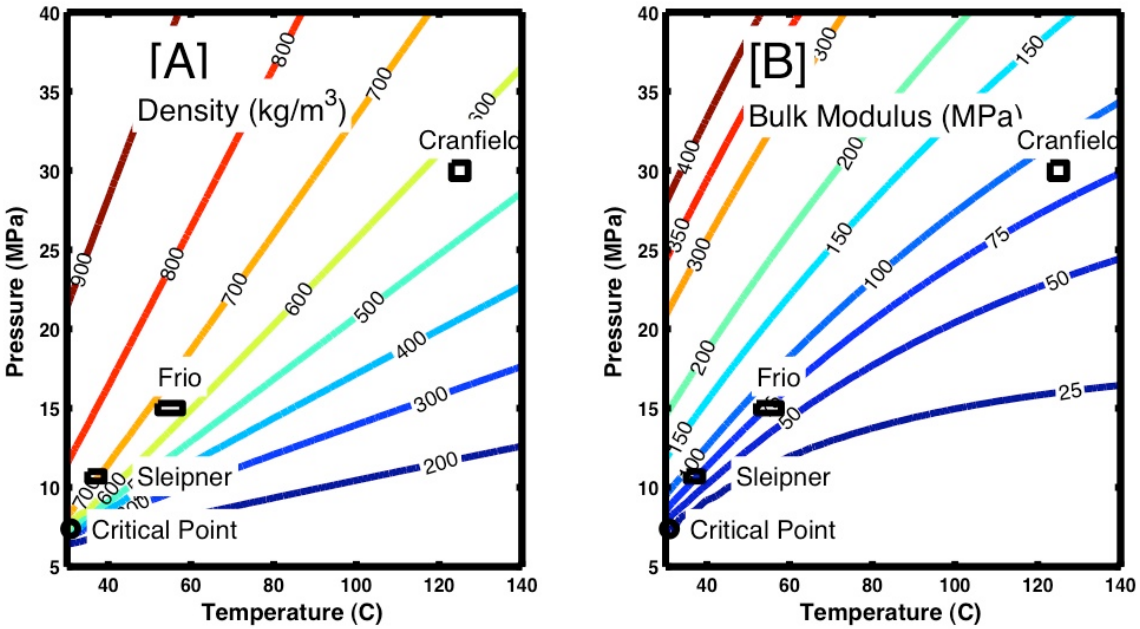

Figure D2. Dependence of CO_2 properties, density and bulk modulus, on pressure and temperature.

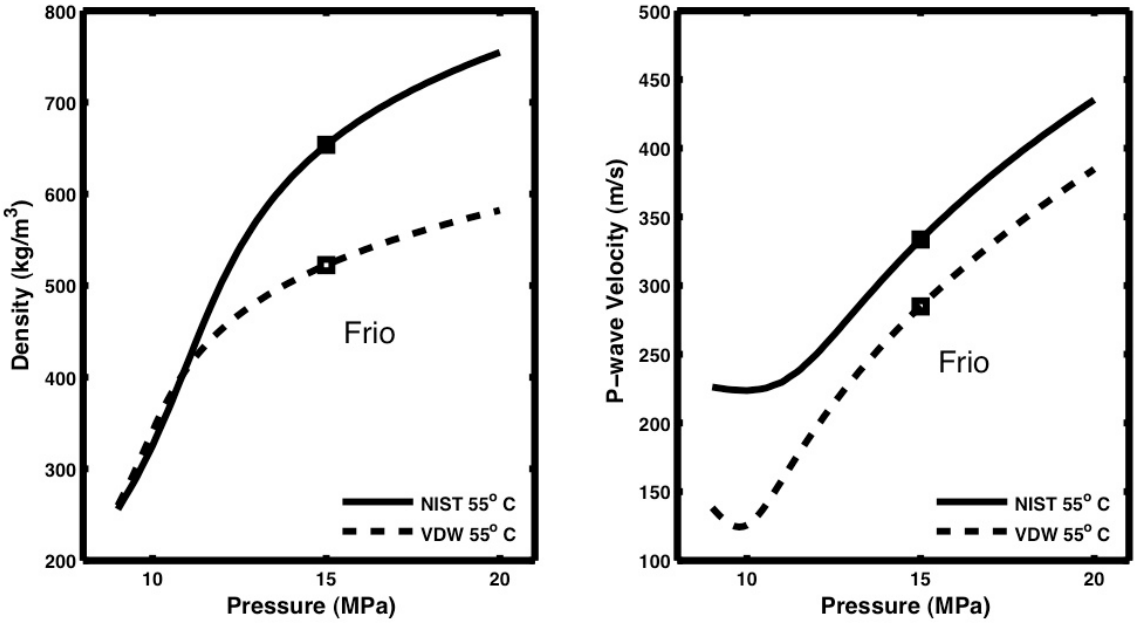

Figure D3. Comparison of NIST data and van der Waals models for CO_2 density and P-wave velocity vs pressure. In-situ Frio conditions show in boxes.

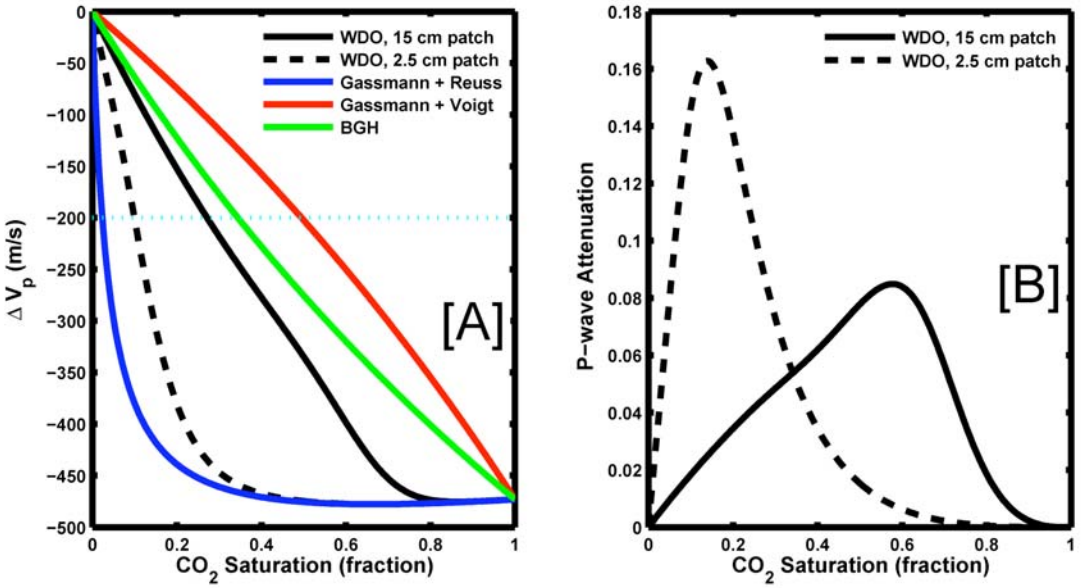

Figure D4. Calculation of change in P-wave velocity (A) and P-wave attenuation (B) for four different poroelastic models. Variation in (A) highlights the importance of using the 'best' rock physics model, i.e., the one most closely corresponding to field conditions.

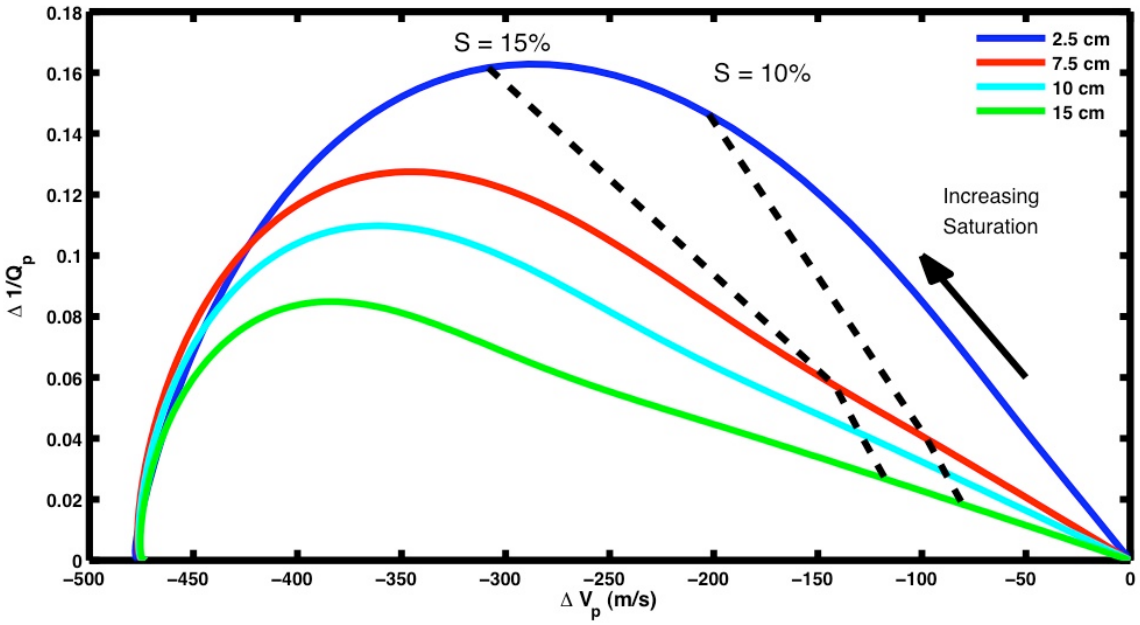

Figure D5. Effect of ”patch” size (colored lines) on seismic velocity (delta V_p) and attenuation (delta $1/Q_p$) is shown as a cross plot. CO_2 saturation is increasing from right to left along the lines as shown by 10% and 15% contours (black dash).